Wave-shaped microfluidic chip assisted point-of-care testing for accurate and rapid diagnosis of infections

Binfeng Yin (binfeng27@hotmail.com)
Yangzhou University https://orcid.org/0000-0002-0484-4951
Xinhua Wan
Yangzhou University
Mingzhu Yang
Chinese Academy of Medical Sciences and Peking Union Medical College Institute of Basic Medical Sciences
Changcheng Qian
Yangzhou University
A S M Muhtasim Fuad Sohan
Yangzhou University

Research

Keywords: POCT, Infection markers, Wave-shaped microfluidic chip, Chemiluminescence, Multiplex detection

Posted Date: October 5th, 2021

DOI: https://doi.org/10.21203/rs.3.rs-829274/v1

Version of Record: A version of this preprint was published at Military Medical Research on February 11th, 2022. See the published version at https://doi.org/10.1186/s40779-022-00368-1.

Abstract

Background: Simultaneous and timely detection of C-reactive protein (CRP), procalcitonin (PCT), and interleukin-6 (IL-6) provides effective information for the accurate diagnosis of infections. Early diagnosis and classification of infections increase the cure rate while decreasing complications, which is significant for severe infections, especially for war surgery. However, traditional methods rely on laborious operations and bulky devices. On the other hand, point-of-care (POC) methods suffer from limited robustness and accuracy. Therefore, it is of urgent demand to develop POC devices for rapid and accurate diagnosis of infections to fulfill on-site militarized requirements.

Methods: We developed a wave-shaped microfluidic chip (WMC) assisted multiplexed detection platform (WMC-MDP). WMC-MDP reduces detection time and improves repeatability through premixing of the samples and reaction of the reagents. We further combined the detection platform with the streptavidin-biotin (SA-B) amplified system to enhance the sensitivity while using chemiluminescence (CL) intensity as signal readout. We realized simultaneous detection of CRP, PCT, and IL-6 on the detection platform and evaluated the sensitivity, linear range, selectivity, and repeatability. Finally, we finished detecting 15 samples from volunteers and compared the results with commercial ELISA kits.

Results: Detection of CRP, PCT, and IL-6 exhibited good linear relationships between CL intensities and concentrations in the range of 1.25-40 μg/mL, 0.4-12.8 ng/mL, and 50-1600 pg/mL. The limit of detection (LOD) of CRP, PCT, and IL-6 were 0.54 μg/mL, 0.11 ng/mL, and 16.25 pg/mL, respectively. WMC-MDP is capable of good adequate selectivity and repeatability. The whole detection procedure takes only 22 minutes that meets the requirements of a POC device. Results of 15 samples from volunteers were consistent with the results detected by commercial ELISA kits.

Conclusion: WMC-MDP allows simultaneous, rapid, and sensitive detection of CRP, PCT, and IL-6 with satisfactory selectivity and repeatability, requiring minimal manipulation. However, WMC-MDP takes advantage of being a microfluidic device showing the coefficients of variation less than 10% enabling WMC-MDP to be a type of POCT. Therefore, WMC-MDP provides a promising alternative to point-of-care testing (POCT) of multiple biomarkers. We believe the practical application of WMC-MDP in militarized fields will revolutionize infection diagnosis for soldiers.

Background

Infections can lead slight skin irritation to severe organ failure if left untreated, especially in the fields of trauma and war surgery. Bacterial and viral infections are the main types of infection. Severe infections can result in sepsis[1, 2]. Delaying an hour in sepsis treatment increases the risk of death by 6-10%[3]. Therefore, it is necessary to use biomarkers for rapid, accurate diagnosis and classification of infections[4-6]. Multiplex detection of C-reactive protein (CRP)[7], procalcitonin (PCT)[8], and interleukin-6 (IL-6)[9] is a reliable method for accurately diagnosing infections and sepsis[10]. In normal human serum, the content of CRP is generally less than 8 μg/mL. The elevation of CRP concentration has a positive

correlation with the severity of infection[11]. CRP increases are typical in bacterial infections and some viral infections like H1N1 and COVID-19[12-14]. Coronary heart disease[15, 16], cancer[17, 18], and other diseases of such kind have high concentrations of CRP. For this reason, it cannot be the primary criterion for diagnosing infections. Normally, blood PCT level is under 0.5 ng/mL for healthy adults. PCT is a specific index for bacterial infection detection[19]. Its concentration will not increase when viral infections occur. IL-6 is a highly sensitive and specific biomarker for infection diagnosis. The level of IL-6 in normal human serum is less than 75 pg/mL[20], which is extremely low. It is hard to detect IL-6 for distinguishing between viral and bacterial infections. In the serum of patients with severe infection or sepsis, the level of IL-6 exceeds 1000 pg/mL. CRP, PCT, and IL-6 have different abnormal times and characteristics. It may lead to the misdiagnosis of infection if only detecting single marker. Multiple detections of CRP, PCT, and IL-6 can cover the whole period of infection. It effectively assesses the classification and severity of infection[21]. It is imperative to develop a multiplex detection technique for infection markers in the fields of militarized point-of-care testing (POCT)[22-24].

As an emerging medical detecting platform, microfluidic chips have the potential to develop militarized POCT devices[25-28]. Mou et al. achieved multiplex detection of CRP, PCT, and IL-6 using electrospun microfibers and gold nanoparticles as signal amplifying methods[29]. The inconvenient steps made the detection take more than an hour. The complicated preparation and instability made it difficult to adapt to the complex environment on battlefields[30]. Russell et al. detected IL-6 in 2.5 minutes with electro-chemiluminescence (ECL) immunoassay[31]. However, it is hard for classificatory diagnosis because of its limitation of a single marker and low sensitivity. Developing a novel microfluidic chip will play a vital role in the classificatory diagnosis of infection throughout existing technologies.

Herein, we report a wave-shaped microfluidic chip (WMC) assisted multiplexed detection platform (WMC-MDP) integrated with micromixer, chemiluminescence (CL), and streptavidin-biotin (SA-B) system for multiplex detection of CRP, PCT, and IL-6. We have developed a novel microfluidic chip with a sandwich structure. WMC consists of a channel layer above, a base layer below, and a detection layer in the middle. Antigens and detection antibodies premix in micromixers. Premix reduces incubation and washing steps cuts of detection time with optimization and pretreatment. SA-B system amplifies the signal of IL-6 to overcome the problem of the large content gap between biomarkers. Application of IL-6 enables detection compatibility with CRP and PCT. We read CL intensity from the CL image analysis system and analyze the contents of biomarkers. WMC-MDP's overall objective is to perform multiple detections for quick analysis of CRP, PCT, and IL-6 in the dynamic battlefield environment for reliably identifying infections.

Methods

Materials and Instruments

Capture antibodies powders of CRP (CRP-Ab_1), PCT (PCT-Ab_1), IL-6 (IL-6-Ab_1) were obtained from Abcam (UK). CRP, PCT, IL-6 were purchased from Abcam (UK). Detection antibodies powders of CRP (CRP-Ab_2), PCT (PCT-Ab_2) conjugated with horseradish peroxidase (HRP) were purchased from Abcam (UK).

Detection antibodies of IL-6 (B-IL-6-Ab_2) conjugated with Biotin and HRP conjugated with SA (SA-HRP) were obtained from Thermo Fisher Scientific (USA). Bovine serum albumin fraction V (BSA) powders were acquired from Tianjin Kangyuan Biotechnology Co., Ltd. (Tianjin, China). Detection antibodies use 0.05% BSA solution to dilute. Pretreating WMC channels requires a 5% BSA solution. Phosphate Buffered Saline (PBS) tablets and Tween-20 were purchased from Amresco (USA) to prepare 0.01 mol/L PBS solution (pH 7.4) and 0.5% Phosphate Buffered Saline Tween-20 (PBST) solution. The capture antibodies and antigens dilute in PBS solution. Supersensitive chemiluminescent substrate reagent kits were obtained from Beijing Labgic Technology Co., Ltd. (Beijing, China). Polydimethylsiloxane (PDMS) and curing agent (Sylgard 184) were purchased from Dow Corning Inc. (USA) to prepare microfluidic chips. Silicone film (100*100*0.1 mm) used to coat capture antibodies was purchased from Shanghai Shentong Rubber and Plastic Products Co., Ltd. (Shanghai, China). Lasty-R resin from SHINING 3D Technology Co., Ltd. (Yangzhou, China) was the material for 3D printing.

Mold manufacturing uses a Lite 600HD 3D printer produced from SHINING 3D Technology Co., Ltd. (Yangzhou, China) DZF-6020A vacuum drying oven, 202-00T electric thermostatic drying were obtained from LICHEN-BX Co., Ltd. (Shanghai, China). SANHOPTT Co., Ltd. (Shenzhen, China) provided PT-10s Plasma Cleaner. ISPLab02 Intelligent syringe pump was acquired from DK INFUSETEK Co., Ltd. (Shanghai, China). CL image analysis system was purchased from BIO-OI Co., Ltd. (Guangzhou, China). Characterization of microchannels uses IMM 3000 metallographic microscopy from MEGA Instruments Co., Ltd. (Suzhou, China). L5S UV/VIS Spectrophotometer from INESA Analytical Instrument Co., Ltd. (Shanghai, China) was to test the transmittance.

Design of the WMC

The sandwich structure design of WMC comprises two parts. Double PDMS layers and a detection layer. It also has additional features containing a valve and two holders. We used SolidWorks® 2016 software to design the three-dimensional model of the WMC.

The channel layer is 68 mm long, 37 mm wide, and 4 mm thick on the top of the sandwich structure. It contains four reservoirs. Each reservoir can accommodate 85 μL reagent. Every reservoir is drilled with a vent of 1 mm in diameter to inject reagents and balance the pressure. A wave-shaped micromixer premixes the antigens, detection antibodies, and enzymes. The mixer consists of five semi-elliptical units of 5 mm on the major axis and 3 mm on the minor axis. Each unit connection has an end-to-end linkage. There is a valve hole between the micromixer and the reservoir of 8.5 mm in diameter to connect them. At the end of the wave-shaped micromixer, we designed detection channels of three linear channels arranged in parallel with a gap of 3 mm. Semicircle channels connect the three linear channels with a negative pressure vent of 1 mm. We inserted all vents into flexible tubes for reagents injection and fluid driving. Thus, allowing both positive and negative pressure for fluid driving. All channels are 400 μm in width and depth with a total fluid holding volume of 20 μL. A silicone film of 10 mm long, 8 mm wide, and 0.1 mm thick is the detection layer coated with capture antibody strips between double PDMS layers. The

bottom base layer of WMC has the same size and valve hole as the channel layer mentioned earlier. There is a waste reservoir designed on the base layer for receiving waste reagents.

The design of the outside chip has two holder plates with a thickness of 2 mm connected by pins to prop up the chip. Both holder plates have holes to fit the translate-type mechanical (TM) valve to avoid the swinging phenomenon of the TM valve. The upper holder plate consists of another hole to expose the vent to the reservoir. TM valve connects the required reservoirs to the wave-shaped micromixer by setting up channels in different heights. During the movement of the TM valve, the connected reservoir is not dependent on the outlet alignment with the corresponding channel on the TM valve.

Fabrication and Assembly of WMC-MDP

The molds of double PDMS layers and auxiliary parts use a 3D printer to manufacture (Additional Fig. S1a) [32, 33]. The molds are made of high-temperature-resistant resin material to avoid mold deformation. It occurs due to high temperature during the curing period of the PDMS. Auxiliary parts made of transparent material can observe the fluid motion conveniently. After printing all the parts, they are washed in an ultrasonic cleaner with 99.7% ethanol for 5 minutes and cured in a UV curing chamber for 15 minutes. We grind the mold to obtain a surface roughness of Ra=1.6 μm. It is conducive for higher dimensional accuracy and transmittance. Gloss oil is sprayed on the surface of the molds to obtain better-shaped channels. PDMS and curing agents are mixed evenly in a weight ratio of 10:1. A vacuum drying oven is used to debubble the mixture. It is then poured into the molds. The PDMS is cured in the electric thermostatic drying oven at 70 ℃ for 90 minutes. After demolding the PDMS, the achievement of the channel layer and base layer are complete. The plasma cleaner breaks the silicon-oxygen bond on the surface and bonds the channel layer and base layer.

We placed the detection layer between the double PDMS layers, necessary precautions to ensure the double PDMS layers can cover the whole detection channels region. The capture antibody strips coated on the detection layer need to be perpendicular to the detection channel. Appling necessary pressure to the double PDMS layers ensures a tight bond. Pins assemble two holder plates to fit the bonded PDMS layers. TM valve is inserted into the valve holes to add samples and drive fluid expediently in the WMC. Flexible tubes of appropriate length are used in all the vents to connect with the pump. Finally, the assembly of WMC-MDP is achieved (Additional Fig. S1b).

Pretreatment of WMC-MDP

All three channels of our microfluidic chip design can coat capture antibodies on the silicone film. The channels are 400 μm in width and depth arranged in parallel at intervals of 3 mm. The silicone film is cut to the design size and placed along the silicone film's length (Additional Fig. S2a). CRP-Ab_1, PCT-Ab_1, IL-6-Ab_1 are injected into the channels respectively and quiescence for 20 minutes (Additional Fig. S2b). Following that, PBST buffer is injected in all channels three times to remove uncoated capture antibodies (Additional Fig. S2c). Finally, removing the chip and obtaining the detection layer coated with captured antibodies strips (Additional Fig. S2d).

50μl 5% BSA solution is added into any reservoir, pressing the TM valve to the corresponding height on the assembled WMC-MDP. The reagents use positive pressure through the reservoir vents or negative pressure through the negative pressure vent to drive. After filling all channels with BSA solution, WMC-MDP is in quiescent for 30 minutes to reduce non-specific adsorption of proteins. Furthermore, the addition of the BSA solution acts as a quality check. If the liquid leaks during the addition process, the chip is of substandard quality (Additional Fig. S3).

Results

Principle

The basic steps of WMC-MDP in detecting CRP, PCT, and IL-6 can be summarized as preprocessing, premixing, and signal readout. Pretreatment involves coating the detection layer with captured antibody strips and modifying the surface of the channels. The purpose of premixing is to mix the antigens with the detection antibodies before conducting an immune reaction. Pre-mixing antigens and detecting antibodies in a micromixer can eliminate the need for incubation and washing, saving half of the detection time. The reaction of the HRP enzyme with the Luminol- H_2O_2 substrate deconstructs H_2O_2 into an oxygen-free radical, which is catalyzed by HRP and oxidizes the luminol to produce CL intensity. The concentration of CRP and PCT are high in serum and can be detected by HRP-conjugated detection antibodies directly. However, due to the low concentration of IL-6 in the serum, we need to introduce a signal amplification method. We used the SA-B system to detect IL-6 by conjugating biotin with detection antibodies and streptavidin with HRP. The preparations of the two conjugates are mature and commercial processes. The CL image analysis system automatically reads CL intensity.

Characterization

The micromixer is a reliable structure integrated with the microfluidic chip[34-36]. The effectiveness of the micromixer lies in evenly mixing the proteins in the samples. This is an essential prerequisite for WMC-MDP to reduce detection time by premixing. We used COMSOL Multiphysics 5.6 software to simulate the mixing condition in the three-dimensional model of the wave-shaped micromixer to explore the mixing effect of reagents in the wave-shaped micromixer. We do not rely on motion changes of an individual protein, so there is no need to consider biomechanical aspects. Driven by the pump, the fluid in WMC-MDP moves at Reynolds numbers (Re) of 0.4 (Fig. 1a), 4 (Fig. 1b), and 40 (Fig. 1c). We set liquid of 0 mol/L and 1 mol/L at the inlet to observe whether the two liquid concentrations could transform into a homogeneous liquid in the wave-shaped micromixer. As the concentration difference decreases, we can observe an excellent mixing effect at the outlet of the wave-shaped micromixer. To quantify the mixing impact, we evaluate the mixing efficiency using the following formula.

$$\sigma = 1 - \sqrt{\frac{\int_{\Gamma}\left(c - \bar{c}\right)^2}{A * \bar{c} * 2}}$$

Where c is the concentration of the liquid, $\bar{c}$ is the average concentration, Γ is the concentration we measured from the outlet plane, A is the area of the outlet plane.

When the Re are 0.4, 4, 40, the resulting mixing efficiencies are 0.99606, 0.99874, and 0.99999. It demonstrates WMC-MDP can perform excellent premixes at a wide range of the Re, and it can satisfy the requirements from manual operations to instrumental automation.

The accurate size is the basis for ensuring the micromixer's normal operation, smooth fluid movement, and accurate detection results. 3D-printed mold is an emerging technology in the manufacture of microfluidic chips[37]. To verify the reliability of manufacturing WMC mold using 3D printing technology, we used microscopy to measure the dimensions of the channels in the WMC. The dimensional deviation of the straight and curved channels in the channel layer (Fig. 2a-c), channel in the TM valve (Fig. 2d) is within 2%. This proves WMC manufactured using 3D printing has extremely high manufacturing accuracy and can meet the requirements of mass production.

In addition to dimensional accuracy, the transmittance is another criterion to evaluate chip manufacturing. To observe the fluid movement in the chip and detect the CL intensity better, we examined the transmittance of WMC in the visible region (380-720 nm) (Additional Fig. S4). The results show the average transmittance of WMC in the visible region is 85.97%. Especially at the optimum detection wavelength of CL (425 nm)[38], the transmittance of WMC is 86.04%. Compared with the 95% transmittance of PDMS, the light transmittance of WMC does not decrease significantly and meets the observation and detection requirements.

Optimization of Coating Capture Antibodies

We coated different capture antibodies concentrations to optimize capture antibodies concentrations of CRP, PCT, and IL-6 onto the detection layer. We investigated CRP-Ab_1 and PCT-Ab_1 of 10 μg/mL, 20 μg/mL, 40 μg/mL, 60 μg/mL, 80 μg/mL (Additional Fig. S5a and b), IL-6-Ab_1 of 20 μg/mL, 40 μg/mL, 60 μg/mL, 80 μg/mL, 120 μg/mL for coating (Additional Fig. S5c). The other experimental conditions are consistent. Initially, CL intensity is positively correlated with the concentration of captured antibodies. After the concentration of captured antibodies rises to a certain extent, the increase of CL intensity becomes inconspicuous. The CL intensity even decreases in a high concentration of captured antibodies. The transition limits of CRP-Ab_1, PCT-Ab_1, IL-6-Ab_1 are 40 μg/mL, 60 μg/mL, and 80 μg/mL. To save expensive reagents, we used the transition limit as the best coating concentration.

Optimization of Detection Antibodies

The optimized concentration of the captured antibodies and the same sample concentration is used to optimize the detection antibodies. The previously mentioned optimization process is used as the reaction

conditions. The detection levels for CRP-Ab2 were 6.25 μg/mL, 12.5 μg/mL, 25 μg/mL, 50 μg/mL, and 75 μg/mL. (Additional Fig. S6a). On the other hand, PCT-Ab_2 and B-IL-6-Ab_2, are investigated with 12.5 μg/mL, 25 μg/mL, 50 μg/mL, 75 μg/mL, 100 μg/mL for detection (Additional Fig. S6b and c). The intensity of CL is enhanced by increasing the detection antibodies concentration until it reaches a plateau after a critical value for achieving the detection antibodies saturation. Therefore, we chose 25 μg/mL of CRP-Ab_2, 50 μg/mL of PCT-$Ab_{2,}$ and B-IL-6-Ab_2 as they proved to be the best concentration.

Detecting Process

We used a negative pressure peristaltic pump to drive the fluid. First, connect the pump to the negative pressure vent. 30 μL of the sample 40 μL mixed solution of the detected antibody and SA-HRP, as well as 70 μL PBST solution and 35 μL CL substrate, are added into the four reservoirs respectively. The concentrations of the biomarkers are calculated based on the final concentration of the sample. This concentration consists of 30 μL detection antibodies mixed with 10 μL, 4 μg/mL SA-HPR and then added into the reservoir (Fig. 3a). The following are the steps of the detection processes: (1) Pressing the TM valve to the appropriate height to ensure the sample and detection antibodies with SA-HRP solution can enter the wave-shaped micromixer. In the micromixer, the reagents can be evenly mixed and initially reacted (Fig. 3b). (2) Pumping the mixed solution into the reaction channel. They are incubated for 20 minutes to generate an immunoreaction, forming a double-antibodies sandwich structure. SA and biotin can also be combined (Fig. 3c). (3) Positioning the TM valve by pressing it to the next height to pump PBST solutions into the detection channel to remove unreacted reagents (Fig. 3d). (4) Pumping CL substrate into detection channel to react with HRP after pressing the TM valve to the last height. The capture antibodies strips and detection channels cross to form a 3*3 detection spots. We obtained the CL intensity by the CL image analysis system and used GEL-PRO Analyzer software for subsequent analysis (Fig. 3e). The entire inspection process takes 22 minutes.

Detecting Performance

Linear range, the limit of detection (LOD), and selectivity can evaluate the detection performance of WMC-MDP. Under these experimental conditions, we detected CRP in the range of 0.16-80 μg/mL, PCT in the range of 0.1-51.2 ng/mL, and IL-6 in the range of 12.5-6400 pg/mL (Fig. 4a and b). CL intensity is linearly related to CRP concentration and ranges from 1.25 to 40 μg/mL for CRP (;). The concentration of PCT has an ideal linear relationship with CL intensity in the range of 0.4-12.8 ng/mL (;). Also, the concentration of IL-6 has an ideal linear relationship with CL intensity in the range of 50-1600 pg/mL (;) (Fig. 4c). The linear range can cover the cut-off value of three biomarkers. , S is the standard deviation of the blank samples, M is the slope of the linear curve. The LOD of CRP, PCT and IL-6 are 0.54 μg/mL, 0.11 ng/mL and 16.25 pg/mL respectively. Since the LOD is far lower than the cut-off value, the sensitivity of the three biomarkers can well meet the needs of POCT.

The premise of WMC-MDP is to realize the multiplex detection of three biomarkers where there are no cross-reactions between them. We detected all the combinations of CRP, PCT, and IL-6 to observe if they

would make a difference (Fig. 4d). The detection process is consistent except for the different combinations of samples in the reservoir. The final concentrations of CRP, PCT and IL-6 are 10 μg/mL, 0.8 ng/mL and 100 pg/mL. The results show the CL intensity can only appear if the corresponding captured antibodies are coated. Different combinations of biomarkers do not affect the CL intensity of the detection spots. It indicates no cross-reactions affect the detection results, and WMC-MDP can carry out the multiplex detection of infection markers.

Reproducibility

Reproducibility is also an important index to evaluate the detection capability of the WMC-MDP. We used ten pieces of WMC produced from the same batch to detect the same sample. The concentrations of CRP, PCT, and IL-6 in the samples are 10 μg/mL, 0.8 ng/mL, and 100 pg/mL. The results show for CRP, the coefficient of variation is 5.24% (Additional Fig S7a). The coefficients of variance for PCT and IL-6 are 5.02% and 6.12 %, respectively (Additional Fig S7b and c). The coefficients of variation of less than 10% indicates the reproducibility of WMC-MDP is compatible for POCT adaptation. The precise fabrication of the WMC and the good optimization of the experimental conditions ensures optimum reproducibility.

Storage Stability

To satisfy the demands of POCT and commercialization, WMC-MDP needs to have excellent storage stability. We investigated the detection capability of WMC-MDP after storing for 1-7 days at a temperature of 4℃ and a pressure of 1 atm. The concentrations of CRP, PCT, and IL-6 to be detected are 10 μg/mL, 0.8 ng/mL, and 100 pg/mL respectively. We found there was no distinct decrease in the WMC-MDP for detecting the same concentration of samples. For CRP, PCT, and IL-6, the coefficients of variation are 6.33%, 5.77%, and 6.64%, less than 15% (Additional Fig S8a-c). It indicates WMC-MDP can stably store the reagents.

Discussion

Clinical Sample Testing

To verify the capability of WMC-MDP to detect human serum samples, we examined 15 clinical samples. By comparing WMC-MDP with commercial ELISA kits, we evaluated the potential of WMC-MDP in practical applications. The results show that WMC-MDP is highly consistent with commercialized ELISA kits in terms of actual samples (CRP, . PCT, . IL-6,) detection (Fig. 5a-f). Samples from 3 healthy people and 12 sick people are all correctly detected. Accurate detection results are the prerequisite for applicating WMC-MDP in disease analysis.

The preset reasonable and uniform cut-off values will facilitate the analysis of clinical samples. We used cut-off values of 8 μg/mL, 0.5 ng/mL, and 75 pg/mL for CRP, PCT, and IL-6, respectively. The cut-off values of biomarkers have certain individual differences and vary from the application. To visually see the changes of biomarkers, we used the fold increase of them compared with the cut-off value to show

the contents of biomarkers (Fig. 5g). From the perspective of patients No.9 and No.15, only the IL-6 level in the patients' blood is higher than the cut-off value. This phenomenon can be because of the time difference in the rise of marker levels. After infection occurs, blood CRP levels begin to rise 6 to 8 hours and peak 24 to 48 hours, PCT levels rise within 2-4 hours and plateau within 12-48 hours, IL-6 levels rise quickly, but the half-life is barely an hour. It indicates the samples may be collected soon after the patient was infected, and IL-6 increases sensitively in the early stages of infection. In contrast, CRP and PCT are not yet elevated. In addition, it is also possible that the infection is caused by a pathogen other than bacteria. Thus, PCT is only sensitive to bacterial infection, while CRP is not sensitive to this pathogen. IL-6 levels are high in patient No. 3, CRP levels are slightly elevated, but PCT levels are normal. Similar to the previous case, it may be because bacteria do not infect the patient, and CRP is sensitive to the pathogen. Medication use may also result in a rapid decline in PCT, which needs further diagnosis according to the patient's medical history. Patient No.8 also aroused our interest in the high levels of CRP and PCT in blood and normal levels of IL-6. This may be because the patient's infection was not severe, and IL-6 levels have declined due to its short half-life, while PCT and CRP have not. The box-and-whisker plot shows infected patients can also have a fold increase of biomarkers levels less than one (Fig. 5h). It means even if a person is infected, concentrations of certain biomarkers may be within the normal range. According to the above case analysis, it is difficult to diagnose infection with an individual biomarker accurately. Multiple detections of CRP, PCT, and IL-6 can fill in the blind area of single marker analysis and accurately diagnose the infection.

Comparison of Detection Capabilities

To verify the detection capability of WMC-MDP, we compared the numbers of biomarkers for detection, detection time, cost, the performance of operations, and LOD value (Table 1). For further verification, we compared all conventional detection methods. So far, WMC-MDP has proven to have a shorter detection time and lower cost. Although the sensitivity of individual biomarkers is not as good as ELISA kits, fluorescence immunoassay, and ECL immunoassay, WMC-MDP is more convenient to use and supports multiple detections of three biomarkers. The great performance of WMC in multiple detections is the cornerstone for the development of military-oriented POCT equipment. However, at the current stage of WMC-MDP, it has deficiencies. For instance, WMC needs to be stored at 4℃ now. It is due to the difficulty of storing the reagents at room temperature. Developing a better reagents storage method is another future research direction for the promotion of WMC-MDP.

Table. 1 Comparison of WMC-MDP detection capabilities.

Detection method	CL	CL	Colorimetric	Fluorescence	ECL
Multiplex detecting	Y	Y	N	Y	N
Detection time	22 min	1 h 10 min	1 h 30 min	33 min	>4 h
Cost	Low	Medium	High	High	Medium
Performance of operations	Simple	Simple	Complicated	Simple	Complicated
LOD					
CRP	0.54 μg/mL	1.87 μg/mL	1.19 μg/mL	5.53 μg/mL	/
PCT	0.11 ng/mL	0.17 ng/mL	0.15 ng/mL	/	/
IL-6	16.25 pg/mL	49.75 pg/mL	12.5 pg/mL	4.41 pg/mL	1 pg/mL
References	This Work	[39]	ELISA KIT	[40]	[41]

Conclusion

In conclusion, to investigate infection in a military scenario, we created a WMC-MDP for multiple detections of CRP, PCT, and IL-6. Antigen and detection antibodies premixing shortens the reaction steps and saves detection time. A dependable manufacturing process and great condition optimization improve the detecting capability and reduce the cost. Pretreatment makes the operation process easier. WMC-MDP has numerous advantages over other detection technologies, particularly in terms of detection time and operating performance. WMC-MDP provides a feasible method for the detection of other pathogens. We believe WMC-MDP can be utilized as a tool for quick infection identification and analysis and it has some potential in the development of militarized POCT devices.

Abbreviations

CRP: C-reactive protein; PCT: procalcitonin; IL-6: interleukin-6; POC: point-of-care; WMC: wave-shaped microfluidic chip; WMC-MDP: wave-shaped microfluidic chip assisted multiplexed detection platform; CL: chemiluminescence; LOD: limit of detection; ECL: electro-chemiluminescence; POCT: point-of-care testing; SA-B: streptavidin-biotin; CRP-Ab_1: capture antibodies of CRP; PCT -Ab_1: capture antibodies of PCT; IL-6-Ab_1: capture antibodies of IL-6; CRP -Ab_2: detection antibodies of CRP; PCT -Ab_2: detection antibodies of PCT; HRP: horseradish peroxidase; B-IL-6-Ab_2: detection antibodies of IL-6 conjugated with biotin; SA-HRP: HRP conjugated with SA; BSA: Bovine serum albumin; PBS: Phosphate Buffered Saline; PBST: Phosphate Buffered Saline Tween-20; PDMS: Polydimethylsiloxane; TM valve: translate-type mechanical valve; Re: Reynolds number.

Declarations

Acknowledgements

The authors thank SHINING 3D Technology Co., Ltd. (Yangzhou and Hangzhou, China) for providing technical support on 3D printing.

Authors' contributions

BFY designed the study, performed the experiments, and provided funding. XHW ran simulations, analyzed the experimental data, and drafted the manuscript. MZY proofread the method and provided funding. CCQ edited graphs and proofread experimental data. ASMMFS revised the manuscript. All authors read and approved the final manuscript.

Funding

This work was financially supported by the National Natural Science Foundation of China (Grant No. 81902167, 52075138), and the Natural Science Foundation of Jiangsu (Grant No. BK20190872).

Availability of data and materials

The data and materials used in the current study are all available from the corresponding author upon reasonable request.

Ethics approval and consent to participate

The studies involving human participants were reviewed and approved by the Ethics Committee of Yangzhou University Medical College. Written informed consent for participation was not required for this study in accordance with the national legislation and the institutional requirements.

Consent for publication

Not applicable.

Competing interests

The authors declare that there are no competing interests.

Author details

[1]School of Mechanical Engineering, Yangzhou University, Yangzhou 225127, China

[2]Department of Biochemistry, Institute of Basic Medical Sciences, Chinese Academy of Medical Sciences (CAMS) & Peking Union Medical College, Beijing 100005, PR China.

References

1. DeMerle KM, Royer SC, Mikkelsen ME, Prescott HC. Readmissions for Recurrent Sepsis: New or Relapsed Infection? Crit Care Med. 2017;45(10):1702-8. https://doi.org/10.1097/ccm.0000000000002626.

2. Ren C, Yao RQ, Ren D, Li Y, Feng YW, Yao YM. Comparison of clinical laboratory tests between bacterial sepsis and SARS-CoV-2-associated viral sepsis. Military Med Res. 2020;7(1):3. https://doi.org/10.1186/s40779-020-00267-3.

3. Marik PE. Don't miss the diagnosis of sepsis! Crit Care. 2014;18(5):3. https://doi.org/10.1186/s13054-014-0529-6.

4. Bao GQ, He L, Lee D, D'Angelo J, Wang HC. An ongoing search for potential targets and therapies for lethal sepsis. Military Med Res. 2015;2(1):20. https://doi.org/10.1186/s40779-015-0047-0.

5. Kumar S, Tripathy S, Jyoti A, Singh SG. Recent advances in biosensors for diagnosis and detection of sepsis: A comprehensive review. Biosens Bioelectron. 2019;124:205-15. https://doi.org/10.1016/j.bios.2018.10.034.

6. Ma XY, Tian LX, Liang HP. Early prevention of trauma-related infection/sepsis. Military Med Res. 2016;3(1):33. https://doi.org/10.1186/s40779-016-0104-3.

7. Yazdanbakhsh K. TRALI: hit by CRP. Blood. 2015;126(25):2661-2. https://doi.org/10.1182/blood-2015-10-675496.

8. Lam SW, Bauer SR, Fowler R, Duggal A. Systematic Review and Meta-Analysis of Procalcitonin-Guidance Versus Usual Care for Antimicrobial Management in Critically Ill Patients: Focus on Subgroups Based on Antibiotic Initiation, Cessation, or Mixed Strategies. Crit Care Med. 2018;46(5):684-90. https://doi.org/10.1097/ccm.0000000000002953.

9. Rose-John S, Winthrop K, Calabrese L. The role of IL-6 in host defence against infections: immunobiology and clinical implications. Nat Rev Rheumatol. 2017;13(7):399-409. https://doi.org/10.1038/nrrheum.2017.83.

10. Reddy B, Hassan U, Seymour C, Angus DC, Isbell TS, White K, et al. Point-of-care sensors for the management of sepsis. Nat Biomed Eng. 2018;2(9):640-8. https://doi.org/10.1038/s41551-018-0288-9.

11. Yeh ETH. CRP as a mediator of disease. Circulation. 2004;109(21 Suppl 1):II11-4. https://doi.org/10.1161/01.CIR.0000129507.12719.80.

12. Wang DW, Hu B, Hu C, Zhu FF, Liu X, Zhang J, et al. Clinical Characteristics of 138 Hospitalized Patients With 2019 Novel Coronavirus-Infected Pneumonia in Wuhan, China. JAMA-J Am Med Assoc. 2020;323(11):1061-9. https://doi.org/10.1001/jama.2020.1585.

13. Chen NS, Zhou M, Dong X, Qu JM, Gong FY, Han Y, et al. Epidemiological and clinical characteristics of 99 cases of 2019 novel coronavirus pneumonia in Wuhan, China: a descriptive study. Lancet. 2020;395(10223):507-13. https://doi.org/10.1016/s0140-6736(20)30211-7.

14. Zhang JN, Zhou LQ, Yang YQ, Peng W, Wang WJ, Chen XL. Therapeutic and triage strategies for 2019 novel coronavirus disease in fever clinics. Lancet Resp Med. 2020;8(3):E11-E2. https://doi.org/10.1016/s2213-2600(20)30071-0.

15. Lloyd-Jones DM, Liu K, Tian L, Greenland P. Narrative review: Assessment of C-reactive protein in risk prediction for cardiovascular disease. Ann Intern Med. 2006;145(1):35-42. https://doi.org/10.7326/0003-4819-145-1-200607040-00129.

16. Lv XX, Wang HD. Pathophysiology of sepsis-induced myocardial dysfunction. Military Med Res. 2016;3(1):30. https://doi.org/10.1186/s40779-016-0099-9.

17. Erlinger TP, Platz EA, Rifai N, Helzlsouer KJ. C-reactive protein and the risk of incident colorectal cancer. JAMA-J Am Med Assoc. 2004;291(5):585-90. https://doi.org/10.1001/jama.291.5.585.

18. Baron JA, Cole BF, Sandler RS, Haile RW, Ahnen D, Bresalier R, et al. A randomized trial of aspirin to prevent colorectal adenomas. N Engl J Med. 2003;348(10):891-9. https://doi.org/10.1056/NEJMoa021735.

19. de Kruif MD, Limper M, Gerritsen H, Spek CA, Brandjes DPM, ten Cate H, et al. Additional value of procalcitonin for diagnosis of infection in patients with fever at the emergency department. Crit Care Med. 2010;38(2):457-63. https://doi.org/10.1097/CCM.0b013e3181b9ec33.

20. Gaini S, Koldkjaer OG, Pedersen C, Pedersen SS. Procalcitonin, lipopolysaccharide-binding protein, interleukin-6 and C-reactive protein in community-acquired infections and sepsis: a prospective study. Crit Care. 2006;10(2):10. https://doi.org/10.1186/cc4866.

21. Pettila V, Hynninen M, Takkunen I, Kuusela P, Valtonen M. Predictive value of procalcitonin and interleukin 6 in critically ill patients with suspected sepsis. Intensive Care Med. 2002;28(9):1220-5. https://doi.org/10.1007/s00134-002-1416-1.

22. Wang P, Kricka LJ. Current and Emerging Trends in Point-of-Care Technology and Strategies for Clinical Validation and Implementation. Clin Chem. 2018;64(10):1439-52. https://doi.org/10.1373/clinchem.2018.287052.

23. Shrivastava S, Trung TQ, Lee NE. Recent progress, challenges, and prospects of fully integrated mobile and wearable point-of-care testing systems for self-testing. Chem Soc Rev. 2020;49(6):1812-66. https://doi.org/10.1039/C9CS00319C.

24. Bissell M, Sanfilippo F. Empowering patients with point-of-care testing. Trends Biotechnol. 2002;20(6):269-70. https://doi.org/10.1016/S0167-7799(02)01961-3.

25. Yang MZ, Liu Y, Jiang XY. Barcoded point-of-care bioassays. Chem Soc Rev. 2019;48(3):850-84. https://doi.org/10.1039/c8cs00303c.

26. Yin BF, Qian CC, Wang SB, Wan XH, Zhou T. A Microfluidic Chip-Based MRS Immunosensor for Biomarker Detection via Enzyme-Mediated Nanoparticle Assembly. Front Chem. 2021;9:11. https://doi.org/10.3389/fchem.2021.688442.

27. Yin BF, Wang Y, Dong ML, Wu J, Ran B, Xie MX, et al. One-step multiplexed detection of foodborne pathogens: Combining a quantum dot-mediated reverse assaying strategy and magnetic separation. Biosens Bioelectron. 2016;86:996-1002. https://doi.org/10.1016/j.bios.2016.07.106.

28. Yin BF, Zheng WS, Dong ML, Yu WB, Chen YP, Joo SW, et al. An enzyme-mediated competitive colorimetric sensor based on Au@Ag bimetallic nanoparticles for highly sensitive detection of disease biomarkers. Analyst. 2017;142(16):2954-60. https://doi.org/10.1039/c7an00779e.

29. Mou L, Dong R, Hu B, Li Z, Zhang J, Jian X. Hierarchically structured microchip for point-of-care immunoassays with dynamic detection ranges. Lab Chip. 2019;19(16):2750-7. https://doi.org/10.1039/c9lc00517j.

30. Ho ZJM, Hwang YFJ, Lee JMV. Emerging and re-emerging infectious diseases: challenges and opportunities for militaries. Military Med Res. 2014;1:21. https://doi.org/10.1186/2054-9369-1-21.

31. Russell C, Ward AC, Vezza V, Hoskisson P, Alcorn D, Steenson DP, et al. Development of a needle shaped microelectrode for electrochemical detection of the sepsis biomarker interleukin-6 (IL-6) in real time. Biosens Bioelectron. 2019;126:806-14. https://doi.org/10.1016/j.bios.2018.11.053.

32. Ho CMB, Ng SH, Li KHH, Yoon YJ. 3D printed microfluidics for biological applications. Lab Chip. 2015;15(18):3627-37. https://doi.org/10.1039/c5lc00685f.

33. Waheed S, Cabot JM, Macdonald NP, Lewis T, Guijt RM, Paull B, et al. 3D printed microfluidic devices: enablers and barriers. Lab Chip. 2016;16(11):1993-2013. https://doi.org/10.1039/c6lc00284f.

34. Lee CY, Fu LM. Recent advances and applications of micromixers. Sens Actuator B-Chem. 2018;259:677-702. https://doi.org/10.1016/j.snb.2017.12.034.

35. Viktorov V, Mahmud MR, Visconte C. Numerical study of fluid mixing at different inlet flow-rate ratios in Tear-drop and Chain micromixers compared to a new H-C passive micromixer. Eng Appl Comp Fluid Mech. 2016;10(1):183-93. https://doi.org/10.1080/19942060.2016.1140075.

36. Raza W, Hossain S, Kim KY. Effective mixing in a short serpentine split-and-recombination micromixer. Sens Actuator B-Chem. 2018;258:381-92. https://doi.org/10.1016/j.snb.2017.11.135.

37. Chan HN, Tan MJA, Wu HK. Point-of-care testing: applications of 3D printing. Lab Chip. 2017;17(16):2713-39. https://doi.org/10.1039/c7lc00397h.

38. Zhou ZM, Yu Y, Zhang MZ, Chen J, Ren QQ, Song JT, et al. Chemiluminescence detection of lead (II) using '8-17' DNAzyme and hemin/G-quadruplex with high sensitivity and selectivity. Sens Actuator B-Chem. 2014;201:496-502. https://doi.org/10.1016/j.snb.2014.05.007.

39. Mou L, Li Z, Qi J, Jiang X. Point-of-Care Immunoassays with Tunable Detection Range for Detecting Infection in Intensive Care Unit. CCS Chemistry. 2021;3(5):1562-72. https://doi.org/10.31635/ccschem.020.202000331.

40. Ruppert C, Kaiser L, Jacob LJ, Laufer S, Kohl M, Deigner HP. Duplex Shiny app quantification of the sepsis biomarkers C-reactive protein and interleukin-6 in a fast quantum dot labeled lateral flow assay. J Nanobiotechnol. 2020;18(1):1-11. https://doi.org/10.1186/s12951-020-00688-1.

41. Li T, Yang M. Electrochemical sensor utilizing ferrocene loaded porous polyelectrolyte nanoparticles as label for the detection of protein biomarker IL-6. Sens Actuator B-Chem. 2011;158(1):361-5. https://doi.org/10.1016/j.snb.2011.06.035.

Figures

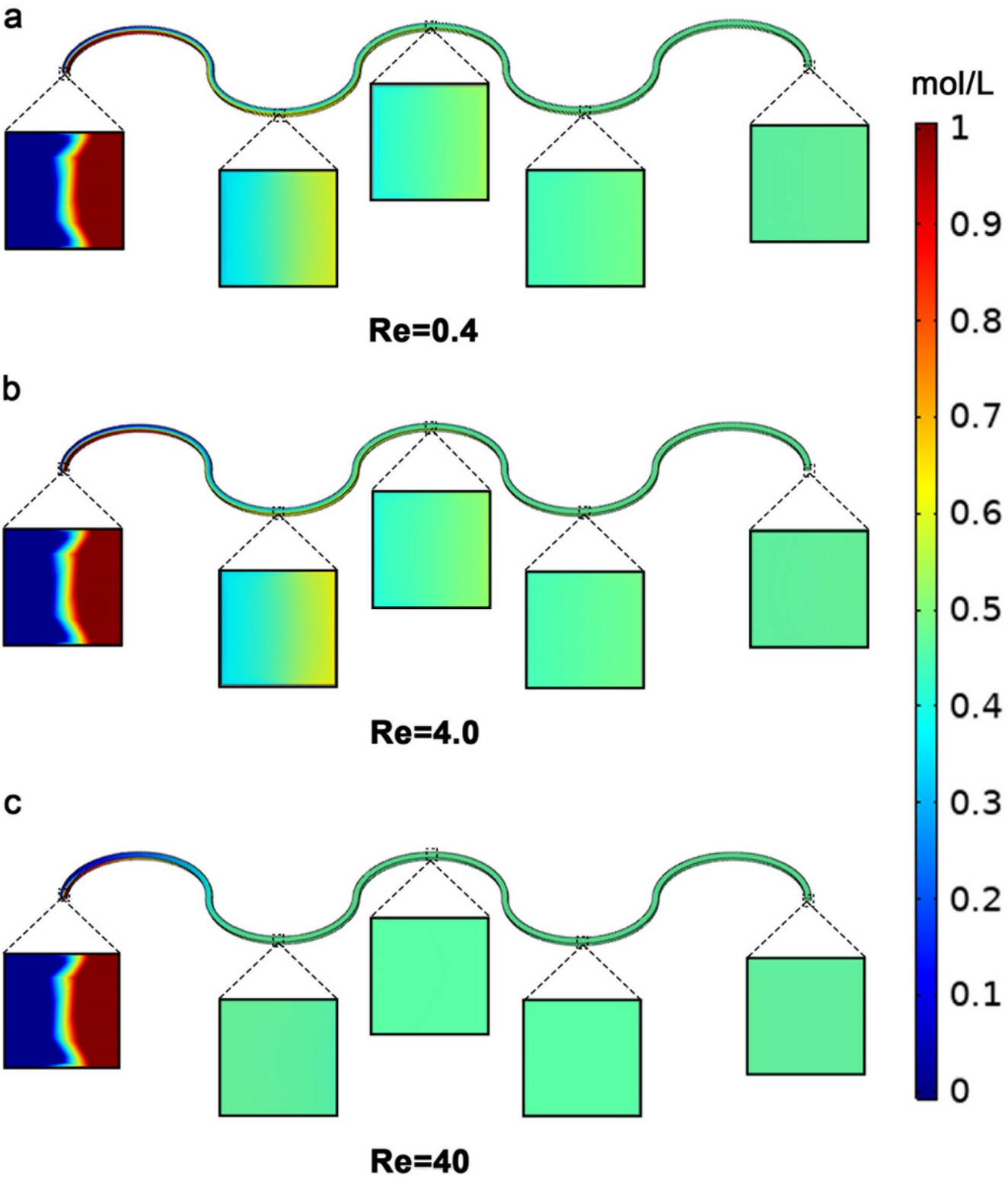

Figure 1

Simulation of the mixing effect of wave-shaped micromixer under different Re using COMSOL software. a. When the Re was 0.4, the mixing efficiency at the outlet was 0.99606. b. Again with the Re of 4 the mixing efficiency at the outlet was 0.99874. c. Under the Re of 40 the mixing efficiency at the outlet observed was 0.99999.

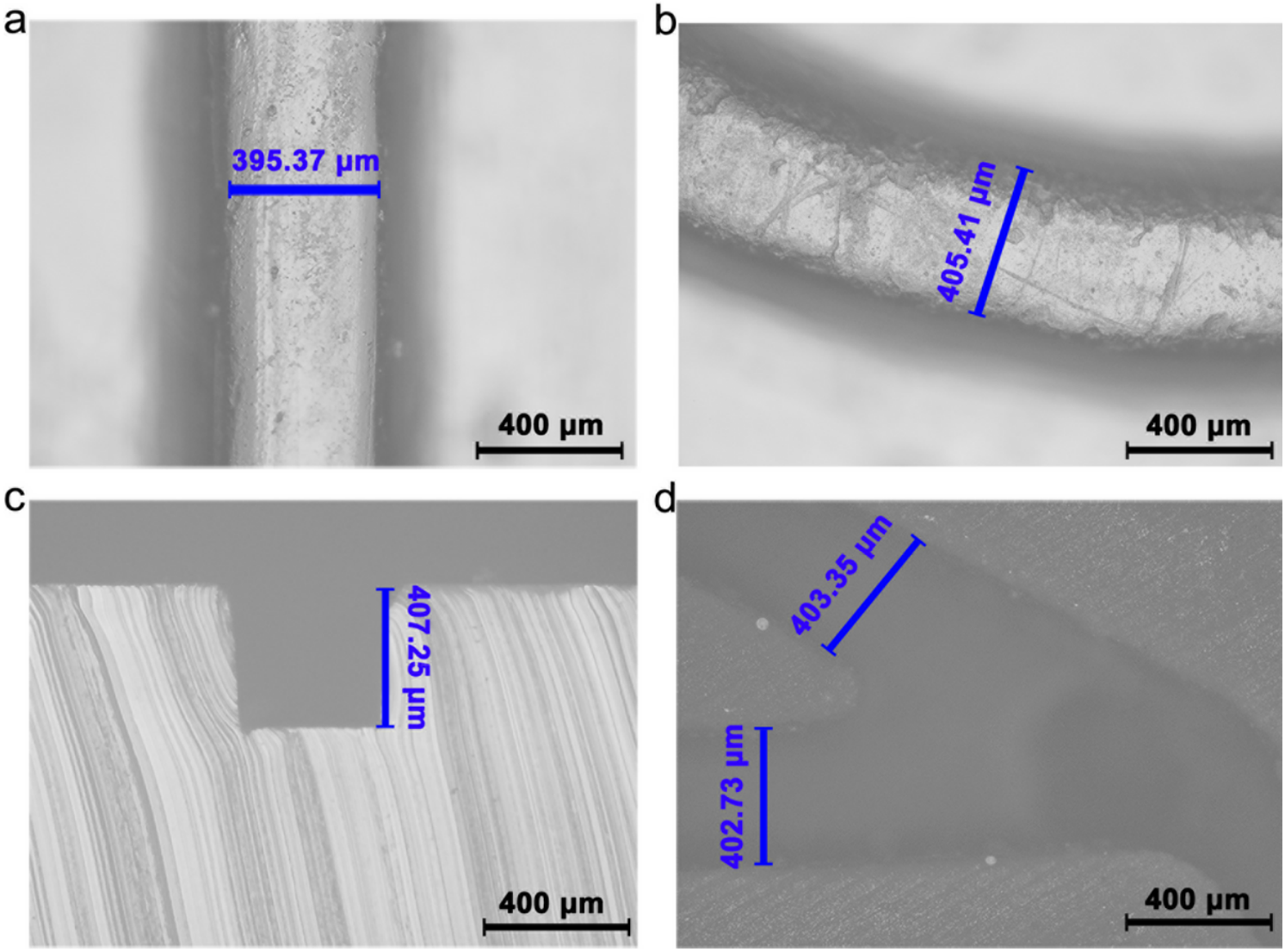

Figure 2

Dimensions of channels in WMC components. a. The WMC microchannels longitudinal part is investigated with the designed width of 400 µm and characterized, and the actual width is 395.37 µm with a dimensional deviation of 1.16%. b. The curved channel of WMC is also measured according to the width design of 400 µm. But the actual width is 405.41 µm, and the dimensional deviation is 1.35%. c. The depth of the channel in WMC has a designed height of 400 µm. But in reality, the height is 407.25 µm with a dimensional deviation of 1.81%. d. Compared with the designed 400 µm width of channels in the TM valve, it has 402.73 µm and 403.35 µm. Here the mean dimensional deviation is 0.61%.

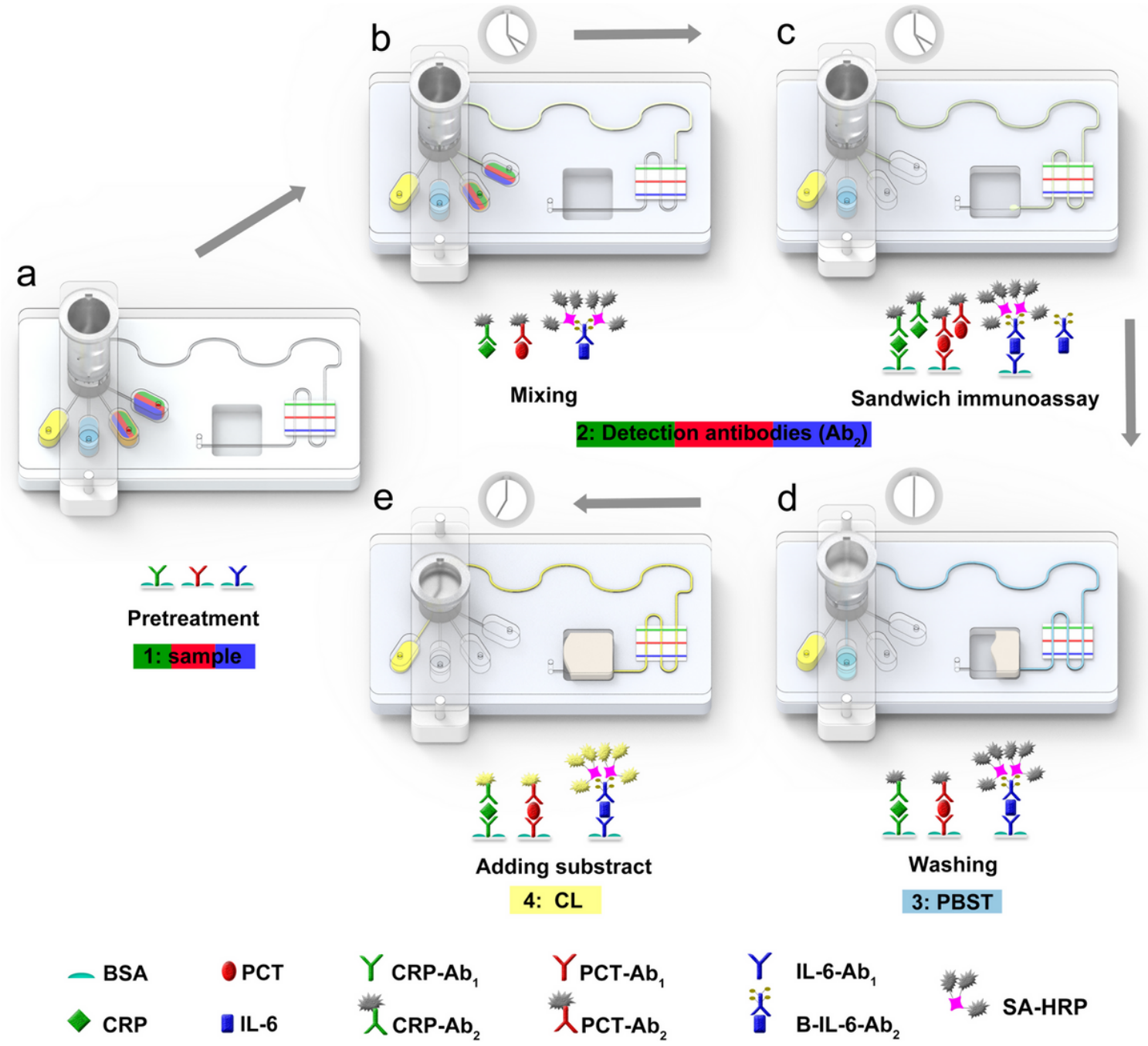

Figure 3

Schematic diagram for multiplex detection of CRP, PCT, and IL-6 using WMC-MDP. a. Prior to detection, pretreatment includes coating capture antibody strips, surface preparation of channels, and the addition of reagents. b. Premixing samples with detection antibodies in wave-shaped micromixer. c. Sandwich immunoassay occurs in the detected channels and forms structures of Ab1-CRP-Ab2-HRP, Ab1-PCT-Ab2-HRP, and Ab1-IL-6-Ab2-B-SA-HRP. d. Removing unreacted reagents by washing channels. e. Adding CL substrate into the channels to produce CL intensity.

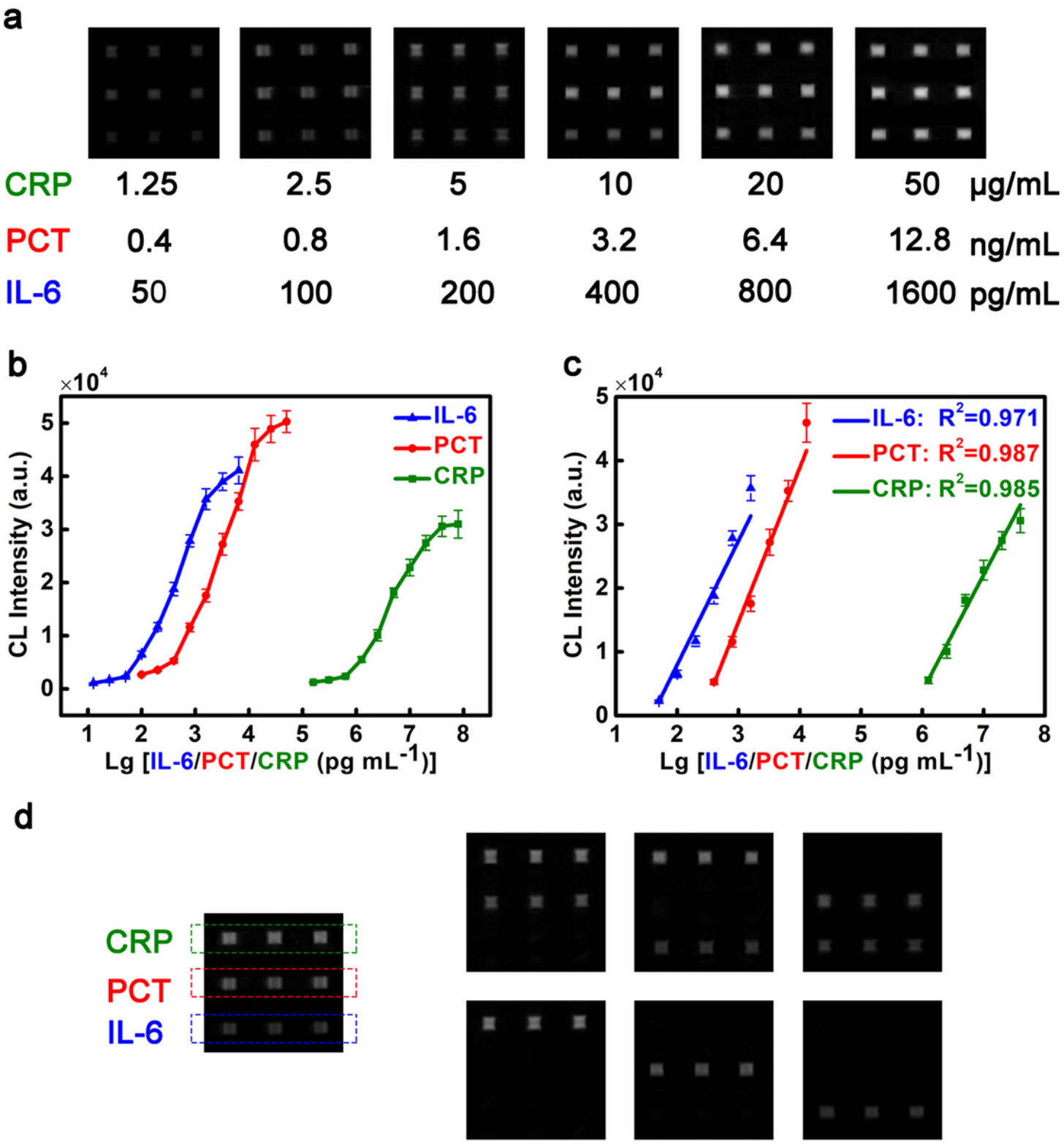

Figure 4

CL intensity is obtained from multiplex detection of CRP, PCT, and IL-6 using WMC-MDP to construct detection range, linear range, and selectivity. a. CL pictures of CRP, PCT, and IL-6 in the linear range at various concentrations. The scan shows CRP in the upper left corner, PCT in the middle, and IL-6 in the lower corner. b. Detection range of CRP, PCT, and IL-6. c. Liner range of CRP, PCT, and IL-6. d. CL images of CRP, PCT, and IL-6 in different combinations.

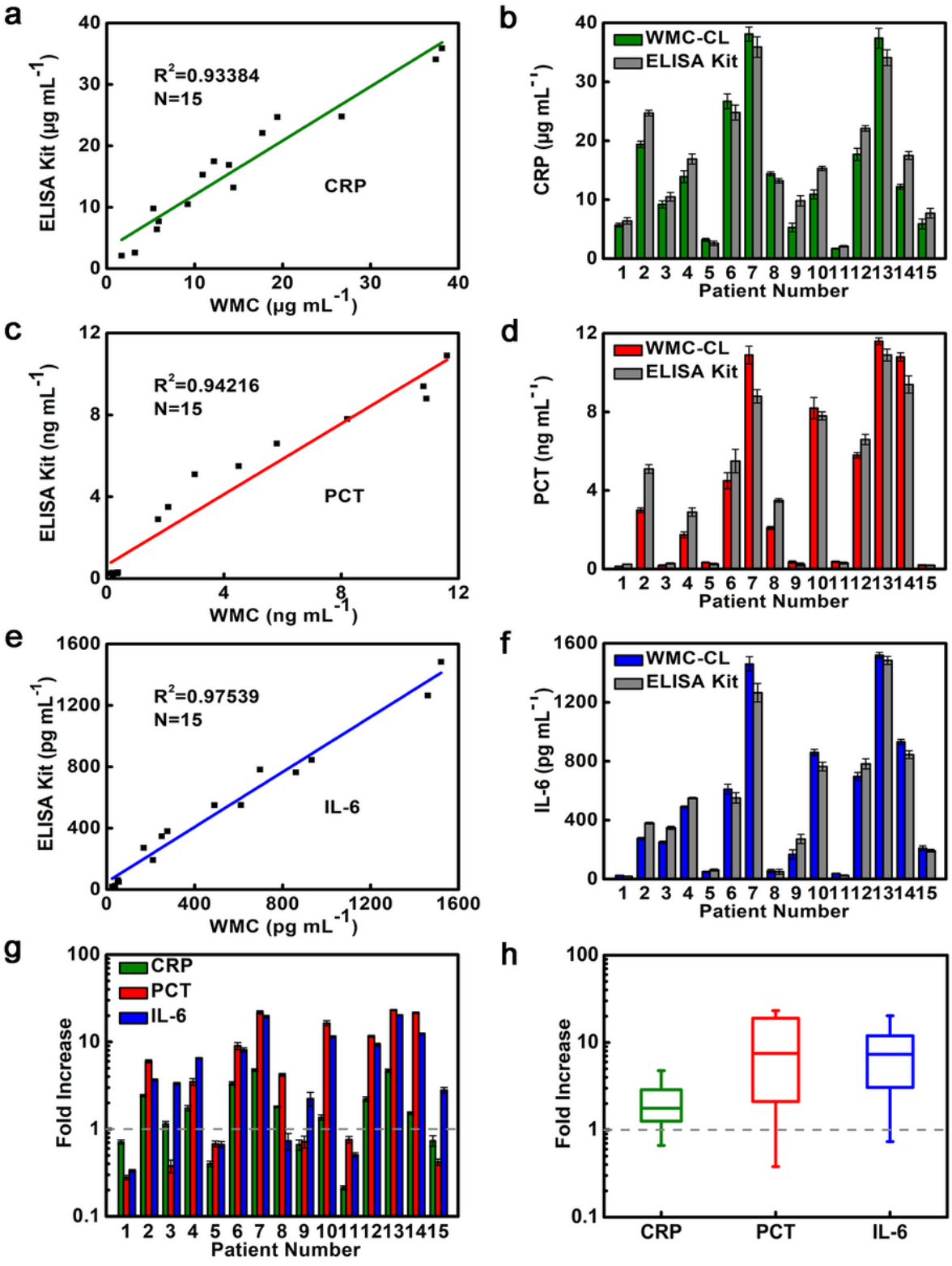

Figure 5

Comparing and analyzing detection data of CRP, PCT, and IL-6 in clinical samples between WMC-MDP and commercial ELISA kits. a-b. Comparison of WMC-MDP and ELISA Kits for CRP detection. c-d. Comparison of WMC and ELISA Kits for PCT detection. e-f. Comparison of WMC-MDP and ELISA Kits for IL-6 detection. g. Analysis of CRP, PCT, IL-6 in clinical samples detected by WMC-MDP. h. Box-and-whisker plot of CRP, PCT, and IL-6 in 12 patients with infection.

Supplementary Files

This is a list of supplementary files associated with this preprint. Click to download.

- SI20210923.docx